Algorithm Theoretical Basis Document
Single Aspirated Air Temperature

PREPARED BY	**ORGANIZATION**	**DATE**
Derek Smith	FIU	02 Jul 2013
Josh Roberti	FIU	02 Jul 2013
Robert Clement	FIU	10 Feb 2010

APPROVALS (Name)	**ORGANIZATION**	**APPROVAL DATE**

RELEASED BY (Name)	**ORGANIZATION**	**RELEASE DATE**

Change Record

REVISION	DATE	ECO #	DESCRIPTION OF CHANGE
A	Jan 2013		Initial Release

TABLE OF CONTENTS

1 DESCRIPTION

Contained in this document are details concerning temperature measurements made at all NEON sites. Specifically, the processes necessary to convert "raw" sensor measurements into meaningful scientific units and their associated uncertainties are described. Temperature will be continuously monitored by NEON at core and relocatable sites by two methods. Temperature for the top of the tower will be derived from the triple redundant aspirated air temperature sensor and will be discussed in additional documents. This document focuses on the Single Aspirated Air Temperature Sensors (SAATS) that will be used to develop temperature profiles. Temperature profiles will be ascertained by deploying SAATS at various heights on the core tower infrastructure and mobile platforms.

1.1 Purpose

This document details the algorithms used for creating NEON Level 1 data product for a single SAATS from Level 0 data, and ancillary data as defined in this document (such as calibration data), obtained via instrumental measurements made by the SAATS. It includes a detailed discussion of measurement theory and implementation, appropriate theoretical background, data product provenance, quality assurance and control methods used, approximations and/or assumptions made, and a detailed exposition of uncertainty resulting in a cumulative reported uncertainty for this product.

1.2 Scope

The theoretical background and entire algorithmic process used to derive Level 1 data from Level 0 data for the SAATS are described in this document. The temperature sensor employed is the Thermometrics Climate RTD 100 Ω Probe, which is housed in a Met One 076B fan aspirated radiation shield to reduce error from direct and indirect radiation. This document does not provide computational implementation details, except for cases where these stem directly from algorithmic choices explained here.

2 RELATED DOCUMENTS AND ACRONYMS

2.1 Applicable Documents

AD[01]	NEON.DOC.000001	NEON OBSERVATORY DESIGN
AD[02]	NEON.DOC.005003	NEON Scientific Data Products Catalog
AD[03]	NEON.DOC.005004	NEON Level 1-3 Data Products Catalog
AD[04]	NEON.DOC.005005	NEON Level 0 Data Products Catalog
AD[05]	NEON.DOC.000782	ATBD QA/QC Data Consistency
AD[06]	NEON.DOC.011081	ATBD QA/QC plausibility tests
AD[07]	NEON.DOC.000783	ATBD De-spiking and time series analyses
AD[08]	NEON.DOC.000746	Evaluating Uncertainty (CVAL)
AD[09]	NEON.DOC.000302	C^3 Single Aspirated Air Temperature
AD[10]	NEON.DOC.000723	Triple Point Temperature Calibration Fixture
AD[11]	NEON.DOC.002002	Engineering Master Location Sensor Matrix
AD[12]	NEON.DOC.000784	ATBD Profile Development
AD[13]	NEON.DOC.000785	TIS Level 1 Data Products Uncertainty Budget Estimation Plan
AD[14]	NEON.DOC.000751	CVAL Transfer of standard procedure
AD[15]	NEON.DOC.000927	NEON Calibration and Sensor Uncertainty Values
AD[16]	NEON.DOC.001113	Quality Flags and Quality Metrics for TIS Data Products

2.2 Reference Documents

RD[01]	NEON.DOC.000008	NEON Acronym List

RD[02]	NEON.DOC.000243	NEON Glossary of Terms

2.3 Acronyms

Acronym	Explanation
ATBD	Algorithm Theoretical Basis Document
CVAL	NEON Calibration, Validation, and Audit Laboratory
DAS	Data Acquisition System
DP	Data Product
GRAPE	Grouped Remote Analog Peripheral Equipment
L0	Level 0
L1	Level 1
N/A	Not Applicable
NOAA	National Oceanic Atmospheric Administration
PRT	Platinum Resistance Thermometer
RTD	Resistance Temperature Detectors
SAAT	Single Aspirated Air Temperature
SAATS	Single Aspirated Air Temperature Sensor

2.4 Verb Convention

"Shall" is used whenever a specification expresses a provision that is binding. The verbs "should" and "may" express non-mandatory provisions. "Will" is used to express a declaration of purpose on the part of the design activity.

3 DATA PRODUCT DESCRIPTION

3.1 Variables Reported

Table 1 details the SAATS-related L1 DPs provided by the algorithms disclosed in this ATBD.

Table 1. List of SAATS-related L1 DPs that are produced in this ATBD. Note: For SAATS measurements, the '0XX' in the eighth field of the Data Product ID refers to the vertical location of SAATS. '001' will always refer to the lowest SAATS (i.e., the lowest boom).

Data product	Averaging Period	Units	Data Product ID
1-minute Mean Temperature ($Mean\_T_1$)	1-min	°C	NEON.DXX.XXX.DP1.00002.001.001.0XX.001
1-minute Minimum Temperature (Min_T_1)	1-min	°C	NEON.DXX.XXX.DP1.00002.001.002.0XX.001
1-minute Maximum Temperature (Max_T_1)	1-min	°C	NEON.DXX.XXX.DP1.00002.001.003.0XX.001
1-minute Temperature Variance ($\sigma^2\_T_1$)	1-min	°C^2	NEON.DXX.XXX.DP1.00002.001.004.0XX.001
1-minute QA/QC Temperature Summary ($Qsum\_T_1$)	1-min	N/A	NEON.DXX.XXX.DP1.00002.001.005.0XX.001
1-minute QA/QC Temperature Report ($Qrpt\_T_1$)	1-min	N/A	NEON.DXX.XXX.DP1.00002.001.006.0XX.001
30-minute Mean Temperature ($Mean\_T_{30}$)	30-min	°C	NEON.DXX.XXX.DP1.00002.001.001.0XX.002
30-minute Minimum Temperature (Min_T_{30})	30-min	°C	NEON.DXX.XXX.DP1.00002.001.002.0XX.002
30-minute Maximum Temperature (Max_T_{30})	30-min	°C	NEON.DXX.XXX.DP1.00002.001.003.0XX.002
30-minute Temperature Variance ($\sigma^2\_T_{30}$)	30-min	°C^2	NEON.DXX.XXX.DP1.00002.001.004.0XX.002
30-minute QA/QC Temperature Summary ($Qsum\_T_{30}$)	30-min	N/A	NEON.DXX.XXX.DP1.00002.001.005.0XX.002

3.2 Input Dependencies

Table 2 details the SAATS-related L0 DPs used to produce L1 SAAT DPs in this ATBD.

Table 2. List of SAATS-related L0 DPs that are transformed into L1 SAAT DPs in this ATBD.

Data product	Sample Frequency	Units	Data Product ID
PRT resistance at temperature T (R_t)	1 Hz	Ω	NEON.DXX.XXX.DP0.00002.001.001.001.XXX.001
Flow Rate	TBD	TBD	TBD
Heater Status	State Change	Binary	NEON.DXX.XXX.DP0.00002.001.004.001.XXX.001

3.3 Product Instances

Multiple SAATS will be deployed at tower sites. SAATS will be located on each boom arm below the top of the tower.

3.4 Temporal Resolution and Extent

One- and thirty-minute averages of temperature will be calculated to form L1 DPs.

3.5 Spatial Resolution and Extent

Each SAATS will represent the point at which it is placed on the tower infrastructure. Ultimately, a temperature profile will be developed for each tower site from the array of SAATSs on the tower (see AD[11] for detail on sensor placement for a specific core site, and AD[12] for description of the algorithms used for deriving this profile).

4 SCIENTIFIC CONTEXT

Temperature is one of the most fundamental physical measurements. It is a primary driving factor for countless physical, chemical, and biological processes. Temperature measurements will provide NEON with ancillary data for numerous other environmental measurements.

4.1 Theory of Measurement

Ultimately, temperature is derived from a PRT. Changes in the PRT resistance due to temperature are determined using a four-wire measurement. The four-wire measurement was chosen due to its decreased dependence on cable length and resistors over the four-wire bridge

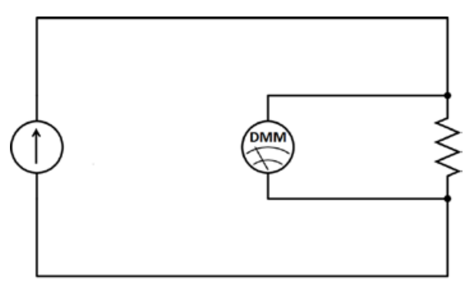

Figure 1. Four-wire measurement for PRT.

method. Using a fixed current source the four-wire measurement detects a voltage drop across a resistor using a digital multi-meter (DMM) with high impedance, shown in Figure 1. The voltage drop across the PRT is used, in conjunction with known current source, to calculate the PRT resistance. This measurement technique accomplished by a DMM (i.e. GRAPE) will acquire resistance for NEON operated PRTs.

4.2 Theory of Algorithm

The PRT is one of the most widely used RTD because platinum has the best linear relationship for changes in resistance to temperature over the greatest temperature range (−200 to 650 °C). Normally, when evaluating temperatures over the entire range of the PRT, the relationship between temperature and resistance for a PRT is expressed by two equations due a divergence from linearity. However, NEON is concerned with only a fraction of the PRT's functional range. Thus, within NEON's desired temperature range the relationship between temperature and resistance is simplified and temperature as a function of resistance is expressed by a single equation (AD[10]):

$$T_i = C_2 {R_{T}}_i^{\,2} + C_1 {R_{T}}_i + C_0 \tag{1}$$

Where:

T_i = Individual (1 Hz) Temperature (°C)
C_0 = Calibration coefficients provided by CVAL (°C)
C_1 = Calibration coefficients provided by CVAL (°C/Ω)
C_2 = Calibration coefficients provided by CVAL (°C/Ω^2)
${R_{T}}_i$ = Individual (1 Hz) resistance at temperature T (Ω)

After resistance is converted to temperature one-minute ($\bar{T}_1$) and thirty-minute ($\bar{T}_{30}$) averages of temperature will be determined accordingly to create L1 SAAT DPs:

$$\bar{T}_1 = \frac{1}{n}\sum_{i=x}^{n} T_i \tag{2}$$

where, for each minute average, n is the number of measurements in the averaging period T, which is defined as 0 ≤ T < 60 seconds.

and

$$\bar{T}_{30} = \frac{1}{n}\sum_{i=x}^{n} T_i \qquad (3)$$

where, for each thirty-minute average, *n* is the number of measurements in the averaging period T and averaging periods are defined as 0 ≤ T < 1800 seconds.

Note: The beginning of the first averaging period in a series shall be the nearest whole minute less than or equal to the first timestamp in the series.

5 ALGORITHM IMPLEMENTATION

Data flow for signal processing of L1 DPs will be treated in the following order.

1. 1 Hz resistance data will be converted to temperature, T_i, according to Eq. (1) using PRT calibration coefficients provided by CVAL.
2. QA/QC Plausibility tests will be applied to the data stream in accordance with AD[06], details are provided below.
3. Signal de-spiking and time series analysis will be applied to the data stream in accordance with AD[07].
4. One- and thirty-minute temperature averages will be calculated using Eq. (2) and (3).
5. Descriptive statistics, i.e. minimum, maximum, and variance, will be determined for both one- and thirty-minute averages.
6. QA/QC consistency tests will be applied to one- and thirty-minute averages in accordance with AD[05].
7. QA/QC Summary (Q_{sum}) will be produced for one- and thirty-minute averages according to AD[16].

QA/QC Procedure:

1. **Plausibility Tests** AD[06] – All plausibility tests will be determined for the SAAT. Test parameters will be provided by FIU and maintained in the CI data store. All plausibility tests will be applied to the sensor's converted L0 DPs and associated quality flags (QFs) will be generated for each test.

2. **Sensor Flags** – Sensor flags (i.e., flow rate and heater) are derived from L0 data products identified in the C^3 document (AD[09]). Any L0 DP (i.e., 1 Hz data) to which the heater and flow

rate flags have been applied will not be used to compute L1 DPs. These flags will be combined with the other QA/QC flags and included in the L1 QA/QC summary (details below).

a. Heater:

$$QF_H = \begin{vmatrix} 1 \; if \quad t_i < t < t_i + (1.5 * t_h) \\ \\ 0 \; otherwise \end{vmatrix}$$

Where: t = Current time
t_i = Initial time that the heater turned on
t_h = Amount of time that the heater stays on for one cycle

The heater flag configuration tests for whether the heater is on or was on during the preceding time interval. Data will continue to be flagged after the heater shuts off for half of the time the heater was operating, to allow for heat to dissipate around the aspirated shield. The t_h time is described in AD[09] and kept in the CI data store..

b. Flow Rate:

$$QF_F = \begin{vmatrix} 1 \; if \quad F < F_{min} \\ \\ 0 \; otherwise \end{vmatrix}$$

Where: F = Flow rate
F_{min} = Minimum flow rate

The flow rate flag indicates whether the sensor is adequately aspirated. F_{min} is a site specific variable that is described in AD[09], provided by ENG, and kept in the CI data store.

3. **Signal Despiking and Time Series Analysis** – Time segments and threshold values for the automated despiking QA/QC routine will be specified by FIU and maintained in the CI data store. QFs from the despiking analysis will be applied according to AD[07].

4. **Consistency Analysis** – A QF for data consistency (QF_V) will be applied according to the consistency analysis outlined in AD[05], and a pass/fail flag will be generated to reflect this activity. To evaluate temperature for consistency, L1 temperature from a given SAATS will first be compared to the SAATS above it on the tower infrastructure. If a difference between the two temperature measurements is less than the defined limits, provided by FIU and maintained in the CI data store, then the sensor will have passed the consistency analysis. Alternatively, a temperature difference between the SAATS outside the defined limits will result in a failed test. A failed test from the above sensor will result in the SAATS being compared to the SAATS below it; if this too results in a failed test then the SAATS will have failed the consistency test and be flagged as such. If the SAATS fails the first test but passes the second then it will have passed the consistency test. This structure helps to ensures that non-functional sensors (e.g. sensors that are faulty or down for service) do not bias the test, since a resulting failed test will allow the sensor to be compared to the one below it. Accordingly, the SAATS on the bottom of the tower will only be compared to the SAATS above it and the uppermost SAATS will first be compared to the TRAATS and then to the SAATS below it. L1 DPs that fail the consistency analysis will continue to be reported, but will have an associated failed QF that will be include in the QA/QC summary.

5. **Quality Flags (QFs) and Quality Metrics (QMs)** AD[16] – If a datum has one of the following flags it will not be used to create a L1 DP, $\underline{QF_R}$, $\underline{QF_D}$, and $\underline{QF_H}$. α and β QFs and QMs will be determined for the following flags QF_R, QF_σ, QF_δ, QF_S, QF_N, QF_G, QF_D, and QF_H. All L1 DPs will have an associated final quality flag, QF_{NEON}, and quality summary, Qsum, as detailed in AD[16]. Flags that may be associated with SAAT's measurements, as well as information maintained in the CI data store can be found below in Tables 3 and 4.

Table 3. Flags associated with SAATS measurements.

Tests	Flags
Range	QF_R
Sigma (σ)	QF_σ
Delta (δ)	QF_δ
Step	QF_S
Null	QF_N

Gap	QF_G
Signal Despiking and Time Series Analysis	QF_D QF_o QF_I
Sensor Test (Heater Flag) AD[09]	QF_H QF_F
Consistency Analysis	QF_V
Final quality flag	QF_{NEON}

Table 4. Information maintained in the CI data store for SAATS.

Tests/Values	CI Data Store Contents
Range	Minimum and maximum values
Sigma (σ)	Time segments and threshold values
Delta (δ)	Time segment and threshold values
Step	Threshold values
Null	Test limit
Gap	Test limit
Signal Despiking and Time Series Analysis	Time segments and threshold values
Calibration	CVAL sensor specific calibration coefficients
Uncertainty	AD[15]
Sensor Test	QF_F and QF_H as described in AD[09]
Consistency Analysis	Test limits
Final Quality Flag	AD[16]

6 UNCERTAINTY

Uncertainty of measurement is inevitable (JCGM 2008, 2012; Taylor 1997). It is crucial that uncertainties are identified and quantified to determine statistical interpretations about mean quantity and variance structure; both are important when constructing higher level data products (e.g., L1 DP) and modeled processes. This portion of the document serves to identify, evaluate, and quantify sources of uncertainty relating to L1 mean SAAT DPs. It is a reflection of the information described in AD[13], and is explicitly described for the SAAT assembly in the following sections.

6.1 Uncertainty of Temperature Measurements

Uncertainty of the SAAT assembly is discussed in this section. Sources of uncertainties include those arising from the calibration procedures, the PRT sensor, heater, aspiration, and measurement noise (Figure 2).

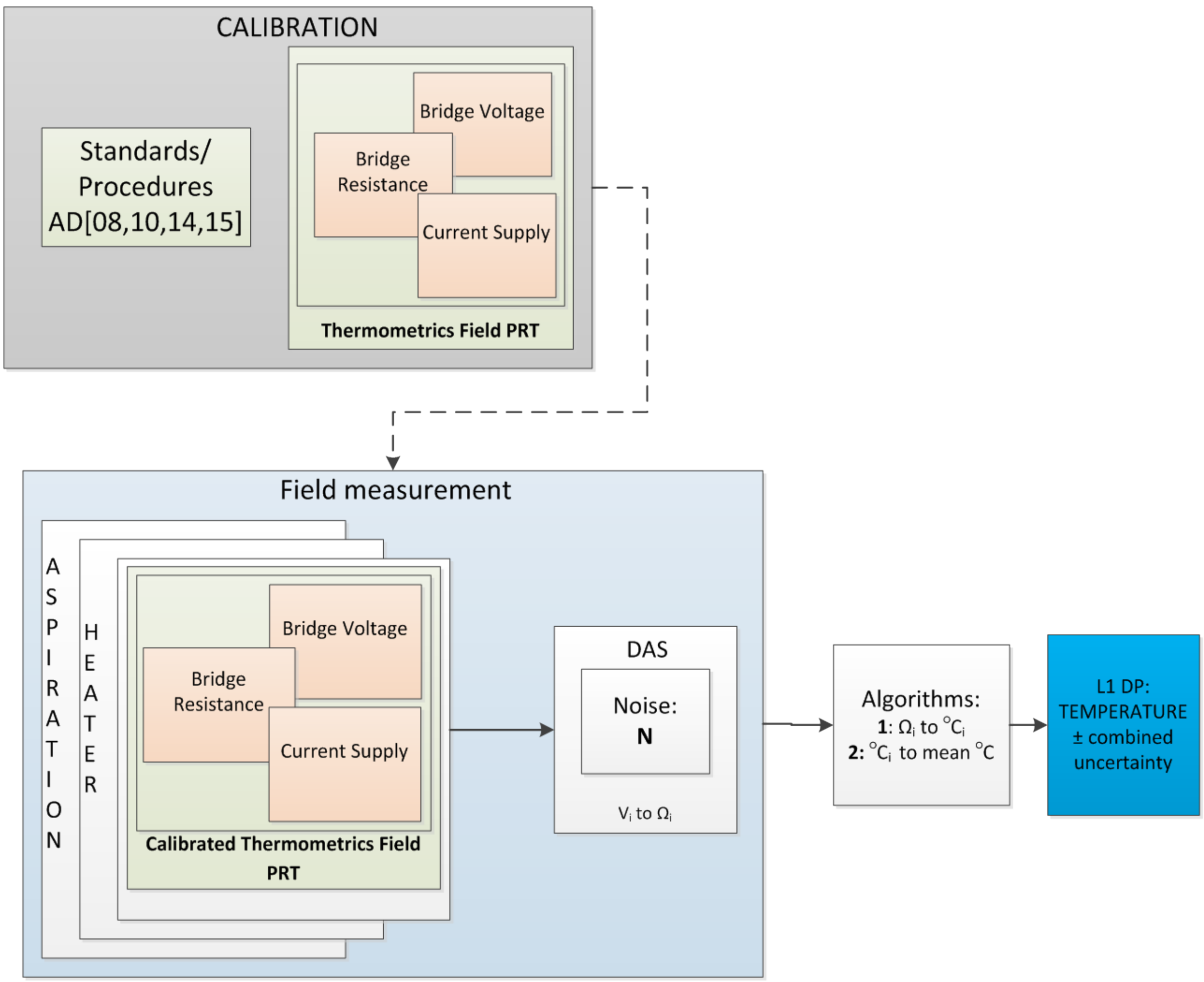

Figure 2: Displays the data flow and associated uncertainties of L1 mean SAAT DPs. Salmon colored boxes represent direct measurement of temperature based on the theory of PRT resistance. For a detailed explanation of the PRT calibration procedures, please refer to AD[08,10,14,15].

6.1.1 Calibration

Uncertainties associated with PRTs and their calibration processes are combined into an individual, standard uncertainty $u_c(T_{CVAL})$ by CVAL. This combined uncertainty represents i) the variation of an individual sensor from the mean of a sensor population, ii) uncertainty of the calibration procedures and iii) uncertainty of coefficients used to convert resistance to calibrated station temperature (refer to Eq. (1)). It is a constant value that will be provided by CVAL (AD[15]), stored in the CI data store, and applied to all PRT measurements (that is, it does not vary with any specific sensor, DAS component, etc.).

6.1.2 DAS

To quantify DAS noise, a *relative* uncertainty value, $u_r(\mathrm{R}_{DAS})$ will be provided by CVAL and stored in the CI data store. This value must be converted into a *standard* uncertainty value:

$$u\left(\mathrm{R}_{DAS_i}\right) = \left(u_r(\mathrm{R}_{DAS}) * R_{T_i}\right) + O_{DAS} \quad [\Omega] \tag{4}$$

Where $u\left(\mathrm{R}_{DAS_i}\right)$ represents the standard uncertainty of an *individual,* raw, resistance measurement, R_{T_i}, and O_{DAS} is the offset imposed by the DAS. The offset accounts for readings of 0.00 Ω; its value will be provided by CVAL and maintained in the CI data store. This individual, standard uncertainty is then multiplied by the absolute value of Eq. (1)'s partial derivative:

$$\frac{\partial T_i}{\partial R_{T_i}} = 2C_2 R_{T_i} + C_1 \tag{5}$$

$$u_{R_T}(T_i) = \left|2C_2 R_{T_i} + C_1\right| u\left(R_{T_i}\right) \quad [°\mathrm{C}] \tag{6}$$

Where, $u\left(R_{T_i}\right) \equiv u\left(\mathrm{R}_{DAS_i}\right)$

6.1.3 Heater

Throughout NEON's Observatory, the exteriors of aspirated shields are partially wrapped in heating material. This material will be turned on during times when ice buildup causes a potential threat to the aspiration within the shield. When the heater is on, it is hypothesized that a portion of the thermal energy will conduct through the aluminum shield, thus altering the internal temperature of the shield and result in large measurement errors.

At this time, the extent to which the heater will affect the measurement uncertainty is unclear. Because of this, any measurements recorded during times of heating, and for a specified time after the heater is turned off (refer to Section 5), will be flagged. This is an example of an uncertainty that can be identified, but cannot be quantified at this time.

6.1.4 Aspiration

The WMO (2006) argues that aspirated shields result in more accurate temperature measurements than naturally ventilated (passive) shields. However, aspirated shields offer minimal natural ventilation given their design (i.e., non-perforated sides hinder natural ventilation), and large temperature errors may be possible if aspiration ceases.

Met One (1997) states that their 076B aspirated shield minimizes temperature errors to $< 0.05\ °F \approx 0.028$ °C, if flow rate within the shield is $500\ F^3\ min^{-1} \approx 0.236\ m^3\ s^{-1}$. This statement may be somewhat misleading, as Met-One hints that temperature errors are *solely* a function of aspiration. However, studies involving both passively ventilated and fan-forced (aspirated) shields show that temperature errors are a function of ventilation/aspiration *and insolation* (e.g., Brock *et al*. 1995; Lin *et al*. 2000; Tarara and Hoheisel 2007). Brock *et al*. (1995) noted that when ventilation fell below 2 m s^{-1} and insolation rose above 700 W m^2, temperature errors were > 2°C for multi-plate, passively ventilated shields. Tarara and Hoheisel (2007) found that non-perforated, tube-shaped, aspirated shields were prone to larger temperature errors than naturally ventilated shields when aspiration/ventilation ≤ 1 m s^{-1} and insolation ≥ 600 W m^{-2}. On the contrary, the authors also showed that temperature errors were *negligible* when ventilation/aspiration was ≤ 1 m s^{-1} and insolation < 200 W m^{-2}, for any type of shield, whether passively ventilated or aspirated. These findings suggest that it may be inappropriate to assign an aspiration rate independent of insolation.

Given the findings of the previous authors it seems plausible that large temperature may be possible if aspiration of Met One's 076B shield completely ceases while insolation is > 200 W m^2. However, the magnitude of these errors is currently unknown. In the future it may be possible to derive sufficient aspiration rates as a function of insolation. For instance, following Tarara and Hoheisel (2007), aspiration ≤ 1 m s^{-1} may be acceptable if insolation is < 200 W m^2, however, aspiration should be ≥ 4.0 m s^{-1} to minimize temperature errors during periods when insolation is ≥ 800 W m^2.

Until NEON data are analyzed and aspiration-insolation correlations are derived for Met One's 076B shield, we are unable to quantify the extent in which temperature measurements will be affected if aspiration reduces or ceases. Until such tests are completed, we will assume that temperatures measured when aspiration is < $0.236\ m^3\ s^{-1}$ are accompanied by an unquantifiable systematic uncertainty. Thus, during these instances, data will be flagged and will not be used to calculate L1 DPs. Even when the flow rate is sufficient, data are still accompanied by a random temperature uncertainty:

$$u(A_s) = \pm\, 0.028\ [°C] \qquad If\ flow\ rate\ \approx\ 0.236\ \mathrm{m^3\ s^{-1}} \tag{7}$$

6.2 Combined Uncertainty

Deriving a combined uncertainty for our L1 mean SAAT DPs can be completed in two steps. Firstly, the combined uncertainty of *individual*, valid (i.e., *those that are not flagged and omitted*) observations made during the averaging period is calculated.

$$u_c(T_i) = \left(u_{R_T}{}^2(T_i) + u_c{}^2(T_{CVAL}) + u^2(A_s)\right)^{\frac{1}{2}} \quad [°C] \tag{8}$$

The resulting value is multiplied by the partial derivative of the L1 DP. Since the DP is a temporal average, the partial derivative is simply:

$$\frac{\partial \bar{T}}{\partial T_i} = \frac{1}{n} \tag{9}$$

Where n represents the number of valid observations made during the averaging period. The absolute value of Eq. (9) is then multiplied by Eq. (8):

$$u_{T_i}(\bar{T}) = \left|\frac{1}{n}\right| u_c(T_i) \quad [°C] \tag{10}$$

Finally, the combined uncertainty of the L1 mean DP is calculated via quadrature:

$$u_c(\bar{T}) = \left(\sum_{i=1}^{n} u_{T_i}{}^2(\bar{T})\right)^{\frac{1}{2}} \quad [°C] \tag{11}$$

Note: In some applications the environmental variation of temperature may be of equal or greater interest than the measurement uncertainty (i.e., combined uncertainty derived in Eq. (11)). While we acknowledge that many approaches exist to quantify environmental variation, listing each method would be lengthy. To promote conciseness we present one method, a simple approach, which describes the variation of the *L1 mean DP* as a function of standard deviation:

$$u(\bar{T}) = \left(\frac{s^2(T_i)}{n}\right)^{\frac{1}{2}} \quad [°C] \tag{12}$$

Where, $s^2(T_i)$ is the variance DP (NEON.DXX.XXX.DP1.00002.001.004.0XX.00X) and n are the number of observations used to generate the DP. It should be noted that such an equation *assumes* the data are normally distributed.

6.3 Expanded Uncertainty

The expanded uncertainty for the L1 mean temperature DP can be derived in a few steps. First, the effective degrees of freedom for each 1 Hz Temperature datum must be computed:

$$V_{eff_{T_i}} = \frac{{u_c}^4(T_i)}{\frac{{u_{R_T}}^4(T_i)}{Veff_{R_{DAS}}} + \frac{{u_c}^4(T_{CVAL})}{Veff_{T_{CVAL}}} + \frac{u^4(A_s)}{Veff_{A_s}}} \tag{13}$$

Where $Veff_{R_{DAS}}$ and $Veff_{T_{CVAL}}$ are functions of the number of tests conducted by CVAL during calibration – their values will be stored in the CI data store; $Veff_{A_s}$ results from a Type B evaluation and its value will be 100 (please refer to AD[13] for further justification).

Second, the effective degrees of freedom must be calculated for our L1 mean temperature DP:

$$V_{eff_{\bar{T}}} = \frac{{u_c}^4(\bar{T})}{\sum_{i=1}^{n}\left(\frac{(u_c(T_i)/n)^4}{V_{eff_{T_i}}}\right)} \tag{14}$$

Finally, the expanded uncertainty is calculated:

$$U_{95}(\bar{T}) = k_{95} * u_c(\bar{T}) \quad [°C] \tag{15}$$

Where k_{95} is the coverage factor obtained with the aid of:

- Table 5 from AD[13]
- $V_{eff}(\bar{T})$

6.4 Uncertainty Budget

The uncertainty budget is a visual aid detailing i) quantifiable sources of uncertainty, ii) means by which they are derived, and iii) the order of their propagation. Individual uncertainty values denoted in this budget are either provided here (within this document) or will be provided by other NEON teams (e.g., CVAL) and stored in the CI data store.

Table 5: Uncertainty budget for L1 mean SAATS DPs. Shaded rows denote propagation (from lightest to darkest) of uncertainties.

Source of uncertainty	**Standard uncertainty component u(X$_i$)**	**Type of eval.**	**Value of standard uncertainty [°C]**	$c_i \equiv \frac{\partial f}{\partial x_i}$	$u_i(Y) \equiv \|c_i\| u(x_i)$ **[°C]**	**Degrees of Freedom**
L1 Temp. DP	$u_c(\overline{T})$	A	Eq. (11)	N/A	N/A	Eq. (14)
1 Hz Temp.	$u_c(T_i)$	A,B[1]	Eq. (8)	Eq. (9)	Eq. (10)	Eq. (13)
Sensor/calibration	$u_c(T_{CVAL})$	AD[15]	AD[15]	1	AD[15]	AD[15]
Noise (DAS)	$u(R_{T_i})$	AD[15]	Eq. (4) [Ω]	Eq. (5)	Eq. (6)	AD[15]
Aspiration	$u(A_s)$	B[1]	Eq. (7)	1	Eq. (7)	100
					k_{95}: $v_{eff_{\overline{T}}}$ & Table 5 of AD[13]	
					$U_{95}(\overline{T})$: Eq. (15)	

[1]Met One (1997)

7 FUTURE PLANS AND MODIFICATIONS

Future system flags may be incorporated into the data stream and included in the QA/QC summary.

8 BIBLIOGRAPHY

Brock, F. V., S. J. Richardson, and S.R. Semmer, (1995) Passive multi-plate solar shields. 9th Symp. Meteor. Obs. And Inst., pp 179-183.

Joint Committee for Guides in Metrology (JCGM) (2008) Evaluation of measurement data – Guide to the expression of uncertainty in measurement. pp. 120.

JCGM (2012) International vocabulary of metrology – Basic and general concepts and associated terms (VIM). 3rd Edition. pp. 92

Lin, X., K. G. Hubbard, and G. E. Meyer, (2000) Airflow Characteristics of Commonly Used Temperature Radiation Shields, Journal of Atmospheric and Oceanic Technology, **18**, pp. 329–339.

Met One Instruments, Inc. (1997) Fan Aspirated Radiation Shield: Specification Sheet. Rev. 076B, pp. 2.

Richardson, S. J., F.V. Brock, S.R. Semmer, C. Jirak, (1999) Minimizing errors Associated with Multi-plate Radiation Shields, Journal of Atmos. And Ocean. Tech., **16**, pp 1862-1872.

Tarara J. M., and Hoheisel G. (2007) Low-cost shielding to minimize radiation errors of temperature sensors in the field. *HortScience*, **42**, 1372-1379

Taylor, J. R. (1997) An Introduction to Error Analysis: The Study of Uncertainties in Physical Measurements. University Science Books, Mill Valley, California. 2nd Ed. pp. 327.

World Meteorological Organization (WMO) (2006) Guide to meteorological instruments and methods of observation: Measurement of Temperature. WMO-No. 8.

9 CHANGELOG